Journal Pre-proof

Modeling soil moisture from *in situ* portable X-ray spectrometer measurements: a novel approach for correcting geochemical data across different environments and climatic conditions

Thomas Vincent Gloaguen, Amélia Paula Marinho Reis, Magali Philippe, Gaël Le Roux

PII: S0883-2927(24)00171-9

DOI: https://doi.org/10.1016/j.apgeochem.2024.106066

Reference: AG 106066

To appear in: *Applied Geochemistry*

Received Date: 21 July 2023

Revised Date: 21 May 2024

Accepted Date: 6 June 2024

Please cite this article as: Gloaguen, T.V., Marinho Reis, A.P., Philippe, M., Le Roux, G., Modeling soil moisture from *in situ* portable X-ray spectrometer measurements: a novel approach for correcting geochemical data across different environments and climatic conditions, *Applied Geochemistry*, https://doi.org/10.1016/j.apgeochem.2024.106066.

Estimation of soil moisture from XRF data

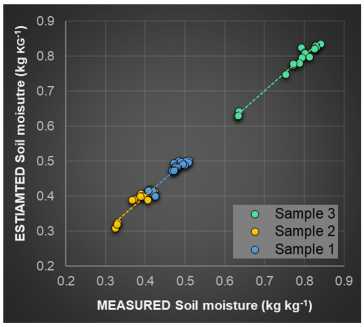

Geochemical mapping of municipality of Estarreja, Portugal

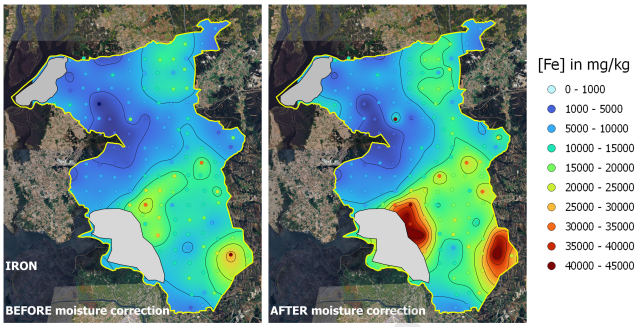

Modeling soil moisture from *in situ* portable X-ray spectrometer measurements: a novel approach for correcting geochemical data across different environments and climatic conditions

Abstract

The portable X-ray fluorescence (pXRF) spectrometer is widely employed for *in situ* analysis of both contaminated and uncontaminated soils. However, the accuracy of the measurements can be significantly affected by soil moisture, resulting in unreliable soil pollution monitoring. This effect has already been studied and quantified, but this is ineffective if the soil moisture in the field is unknown. Given the considerable variability of soil moisture conditions across time and space, significant bias during *in situ* investigations remains a main issue. This study introduces a novel method to estimate soil moisture directly from pXRF field measurements, enabling its reliable use in almost any field condition. The study was conducted using soil samples and *in situ* pXRF soil surface measurements in Estarreja (Portugal) and Vicdessos (France). In the first experiment, the innovative approach involved modeling soil moisture directly from the raw XRF measurement errors obtained in moist soils, using multiple regression. In the second experiment, metal concentrations were modeled as an exponential function of the moisture content. The final model integrates both approaches to correct field data from geochemical mapping in diverse environments, including a coastal region in Portugal and a mountainous region in France. Our findings demonstrate that this simple, efficient and cost-effective method accurately predicts soil moisture (U) using pXRF, as shown by the equation $U_{measured} = 1.0028 \times U_{estimated}$ ($r^2 = 0.9715$). The model effectively corrected up to 70% of moisture-induced errors in metal concentrations in the wettest soils and produced more reliable soil Fe, Pb, and Zn maps. Specifically, the accuracy improvement was at least 32% in drier soils

(Portugal) and at least 55% in wetter soils (France). This study offers a cost-effective, efficient solution for employing pXRF in geochemical mapping across different climatic conditions and soil environments.

Keywords

pXRF; soil pollution; multiple regression model; geochemical mapping

1. Introduction

Over the past decade, the portable X-ray fluorescence spectrometer (pXRF) has emerged as an important instrument for assessing soil contamination (Borges et al., 2020; Caporale et al., 2018; Kallithrakas-Kontos et al., 2016; Parsons et al., 2013; Ravansari et al., 2020; Rouillon and Taylor, 2016). Recently, it has been integrated with other techniques such as Vis-NIR or gamma-ray spectroscopy to improve the prediction of soil attributes (Li et al., 2021; Nawar et al., 2022; Qingya et al., 2022). Some of the advantages of pXRF include its efficiency (analysis in seconds to minutes), reliability, and versatility in analyzing various materials (rocks, soils, organics, metals). Apart from evaluating soil contamination, pXRF finds application in soil geochemistry and mapping (Benedet et al., 2020; Lemière, 2018; O'Rourke et al., 2016a; Stockmann et al., 2016a; Weindorf et al., 2014, 2012; Young et al., 2016).

Nevertheless, the primary challenge lies in the measurement uncertainty due to variable field conditions. Some authors have advised against underestimating metal concentrations using pXRF data and recommend additional soil sampling and geostatistical simulation (Horta et al., 2021; Qu et al., 2022), or other complementary spectroscopy analyses (Li et al., 2021; Shrestha et al., 2022) for more accurate analysis. To mitigate the effects of field conditions during pXRF measurements, several precautions have been reported in the literature, including slight compaction of the soil, removal of organic matter from the surface, and control of soil moisture

(Sharma et al., 2014; Weindorf et al., 2012; Zhu et al., 2011). Compacting soil and removing coarse material is relatively straightforward, while measuring soil moisture can be time-consuming, depending on the method employed. This contrasts with the fundamental principle of XRF, which is designed to quick and practical analyses.

In environmental studies, the impact of soil moisture on XRF measurements is a well-documented concern (Bastos et al., 2012; Kalnicky and Singhvi, 2001; Laiho and Perämäki, 2005; Padilla et al., 2019; Schneider et al., 2016; Stockmann et al., 2016c). Water molecules scatter and absorb primary X-rays, which reduces the signal intensity, particularly in clayey soils with a high Fe content (Ge et al., 2005; Stockmann et al., 2016b). Although some studies have addressed the inaccuracies in data resulting from soil moisture (Akopyan et al., 2018; Argyraki et al., 1997; Bastos et al., 2012; De La Calle et al., 2013; Parsons et al., 2013), most *in situ* geochemical maps do not include a correction for soil moisture. The USEPA Method 6200 suggests that soil moisture content should ideally be below 20% to mitigate the impact on XRF measurements (US Environmental Protection Agency, 2007). However, achieving this condition in the field can be challenging due to regional, climatic, and seasonal variations. Moreover, local variations in moisture across different soil sampling sites can result in unreliable field data. Some researchers have proposed correcting XRF geochemical data in hydromorphic wetland soils by correlating them with laboratory wavelength dispersive X-ray fluorescence (Borges et al., 2020). Alternatively, soil moisture can be measured in the laboratory for post-processing correction, although these methods are time-intensive. Instruments like neutron probes, electrical conductivity-based sensors, or specific moisture probes (Argyraki et al., 1997) are ocasionnaly employed for measuring soil moisture, but they increase study costs and complicate and slow down the *in situ* XRF analysis.

To address these challenges, this study introduces a novel approach for modeling soil moisture directly from the raw field XRF measurement errors. The objective of this method is

to systematically correct measurements at each sampling site, regardless of soil moisture content. This correction method was applied to *in situ* geochemical mapping in two different environments: a mountainous region of the French Pyrenees in more humid conditions, and a coastal region of Portugal in drier conditions.

2. Methodology

2.1. Description of the study area, soil sampling, and mapping

The methodology flow chart is depicted in Figure 1. A soil sampling campaign with *in situ* XRF measurements was conducted at two sites of the French Centre National de la Recherche Scientifique (CNRS), known as Observatoires Homme-Milieu (OHM).

The OHM of Estarreja is situated near the city of Aveiro, Portugal. This area includes the Estarreja Eco Park, one of the Portugal´s largest industrial facilities. Given the presence of numerous plastic factories, metal equipment factories, and chemical plants, this area is significantly contaminated (Barradas et al., 1992; Costa and Jesus-Rydin, 2001; Inácio et al., 2014, 1998; Marinho-reis et al., 2020; Plumejeaud et al., 2018). Geochemical mapping of the entire municipality of Estarreja (108.17 km^2) was performed with a ThermoFisher handheld field X-ray fluorescence analyzer (Niton XL3t – details provided below), on a regular 750 × 750 m grid, with 140 sample sites (1.8 samples/km^2). For each site, the surface soil was analyzed at three sub-sites within a 5 m radius area (each value represents an average of three values). As described in the USEPA Method 6200 (US Environmental Protection Agency, 2007), coarse materials such as leaves, grass, stones, roots, etc., were removed, and the soil was slightly compacted to ensure an adequate contact between the soil and the instrument. The analyzing duration for each sample was 120 seconds.

The second site is the OHM at Vicdessos, located in the French Pyrenees mountain range. The site has a history of contamination due to centuries of lead, zinc, and arsenic ores

exploration (Hansson et al., 2019, 2017; Simonneau et al., 2013). The study focused on valley soils to investigate how runoff, atmospheric deposition, and urban activities contribute to soil contamination. Soil sampling was conducted at 48 sites within this area, resulting in a density of 8 samples/km2. This higher density compared to the sampling density in the OHM in Estarreja is attributed to the greater geodiversity of the region. Additionally, 47 soil samples were collected in the two adjacent Suc-et-Sentenac and Auzat valleys. The sampling and analysis procedures were similar to those used in the OHM of Estarreja.

Regarding the technical characteristics of the ThermoFisher Niton XL3t, its analytical capacity encompasses elements ranging from S to U. It features a small 3 mm sample area, and is equipped with a gold (Au) x-ray tube capable of reaching 50 kV. The system incorporates advanced semiconductor detectors and weighs about 1.3 kilograms.

To ensure the analytical quality of all field and laboratory measurements, nine certified reference materials (BCR141-R, BCR142R, BCR145-R, IAEA-SL1, LKSD-3, RTH912, STSD-3, SUD-1, and WQB1) were used, for obtaining precision (reproducibility of measurements), limits of detection, generating calibration curves, and correcting the dataset. The performance of the instrument is detailed in Table S1 (Supplementary material).

Geochemical maps were generated from field XRF data by analyzing semivariograms for autocorrelation, spatial dependence, and isotropy. The interpolation method used was ordinary kriging, which is more suitable for environmental studies (Goovaerts, 1999). Statistical description, geostatistical analysis, data manipulation, and map production were performed using *SAGA GIS 9.3* and *QGIS 3.28*.

2.2. Correction of XRF data from the modeled soil moisture

To develop a method for estimating soil moisture directly from XRF data, two laboratory experiments were conducted. Subsequently, the method for moisture correction was applied to field data.

2.2.1. Experiment 1: Modeling soil moisture from XRF measurement errors

Twenty percent of the 140 sites (28 samples) were collected during the geochemical mapping survey in Estarreja. Each sample consisted of three sub-samples collected within a radius of five meters. Before sampling a different site, the equipment was thoroughly cleaned with Milli-Q water. Based on particle size analysis of the 28 soil samples in triplicates (Horiba LA950-V2 laser particle analyzer, Table S2, Supplementary material), five soils were selected, ranging from sand to silt texture: sand, sandy loam, silt loam and silt. Soil texture is an important factor influencing infiltration and moisture retention. The five soils were chosen based on their sand content: 10.6% (representing 0-20%), 33.3% (20-40%), 49.0% (40-60%), 70.6% (60-80%), and 87.6% (80-100%). Meanwhile, the clay content in the studied region varied minimally. A chemical analysis of the soil samples is provided in Table S3 (Supplementary material). After air drying at 20°C to 30°C in an isolated room, the soil samples were quartered and sieved (< 2 mm). Triplicate soil samples of defined mass were prepared in vials for XRF analysis (soil height in vial = 7 mm). Milli-Q ultrapure water was meticulously added to the soil until saturation was achieved, and the samples were sealed for overnight equilibration. The following day, the process of soil drying started: after drying at 35 °C for 60 min, the samples were analyzed with the pXRF spectrometer and weighed for calculation of soil moisture. The process was repeated five times. In order to accelerate the evaporation process, the subsequent seven measurements were taken after drying at 60°C for 30 min, and the final two measurements were taken after drying at 105 °C for 10 min (see evolution of the soil moisture during the experiment in Supplementary material, Fig. S1).

149 The innovative approach for modeling soil moisture from XRF data involved considering
150 that the measurement errors from the pXRF spectrometer are substantially affected by soil
151 moisture. Soil moisture was modeled with 70 measurement errors: 5 soil samples at 14 drying
152 stages. The chemical elements were selected based on the correlation between their
153 concentration and soil moisture, and the mathematical model employed was a multiple linear
154 regression (Equation 1).
155
156 $$U_{estimated} = \sum_{i=1}^{n} \beta_i . error_i$$ Equation 1
157 Where
158 $error_i$ is the measurement error of the pXRF spectrometer for the chemical element i
159 β_i is the regression coefficient for element i
160

161 A separated soil samples dataset was exclusively used to validate the accuracy of the model.
162 In conjunction with the XRF field mapping directly on the soil surface, as described previously
163 (section 2.1), soil samples were collected at over 50% of the sites in Estarreja, precisely at the
164 location of the XRF measurement of the soil surface at sub-site R1 (0.5 cm depth,
165 approximately 50 g, n=71). The objective of this secondary sampling was to obtain precise
166 measurements of soil moisture and XRF values in the laboratory. Samples were sealed in Falcon
167 tubes with Teflon tape to prevent moisture loss during storage and transport. After XRF
168 measurements in the laboratory (3 triplicates for each soil sample), the samples were promptly
169 dried at 105°C to measure the exact soil moisture. A theoretical estimated soil moisture was
170 calculated based on the XRF results using Equation 1, after which the measured and the XRF-
171 based estimated moistures were compared.
172

2.2.2. Experiment 2: Modeling the effect of soil moisture on the metal concentration

The second experiment demonstrates the influence of soil moisture on XRF measurements and its effect on attenuating metal concentration values. This effect has already been reported in several studies, but we opted to replicate it with our soils to obtain a more precise final model that incorporates data from both experiments. The metal concentration in dry soil was modeled based on soil moisture and the measured metal concentration in the moist soil (Equation 2). The concentration detection ratio (%C - Equation 3) was derived from Equation 2.

$$[M_i]_{dry\ soil} = e^{\alpha.U}.\ [M_i]_{moist\ soil} \quad \text{Equation 2}$$

$$\%C = 100.\frac{[M_i]_{dry\ soil}}{[M_i]_{moist\ soil}} = 100.e^{\alpha U} \quad \text{Equation 3}$$

Where

$[M_i]_{dry\ soil}$ and $[M_i]_{moist\ soil}$ are the concentrations of the metal i in dry and moist soils, respectively (mg kg^{-1})

U is the gravimetric soil moisture (kg kg^{-1})

α is an estimated empirical constant

The final model (Equation 4) was obtained by combining Equations 1 and 2, and used to correct the field data under moist soil conditions.

$$[M_i]_{dry\ soil} = e^{\alpha.\sum_{i=1}^{n}\beta_i.error_i}.\ [M_i]_{moist\ soil} \quad \text{Equation 4}$$

3. Results and discussion

3.1. Estimation of the soil moisture

Soil moisture not only influences the X-ray measurements, as evidenced by the clear effect in the spectra (Figure 2), but also impacts the accuracy of the measurements, which is represented by the instrument´s measurement errors. The model for estimating of soil moisture from raw pXRF errors (Equation 1) is detailed in Table 1, with an analysis of variance and statistics of the multiple regression model. The coefficient of multiple determination (0.9848) indicates the high accuracy of the model. The estimated soil moisture closely aligns with the measured soil moisture (Equation 2; $U_{measured} = 1.0028 \times U_{estimated}$), with an r^2 of 0.9715 (Figure 3A). The mean difference between estimated and measured moisture was 4.69%, but a T-test showed no significant difference.

To validate the accuracy of our model, we tested it on the 71 field samples (sub-sample R1) collected from different geological units (Quaternary sediments and Proterozoic shales, sandstones, and conglomerates). The model effectively fits the data for different soil moisture contents (Figure 3B). Particularly, at low soil moisture (U < 10%, U_{mean} = 3.1 %), the mean difference between estimated and measured soil moisture was only 1.5%. For the entire dataset, the difference was 4.90%, close to that obtained in the laboratory experiment (4.69%).

Based on these findings from both laboratory and field studies, modeling soil moisture with raw XRF measurements errors demonstred efficacy and precision. The subsequent step involved determining the impact of soil moisture on XRF measurements in our specific soils, and integrating those equations to correct the XRF data.

3.2. Effect of soil moisture on XRF measurements

According to previous studies (Padilla et al., 2019; Schneider et al., 2016; Stockmann et al., 2016b), average metal concentrations typically decline with soil moisture. Our current results

align with this trend, showing a significant decrease in the concentration of Fe, Ca, K, Ti, between 0% and 80% gravimetric moisture (Figure 4). Notably, the moisture effect is more pronounced in soils with higher metals concentrations, as evidenced by the data for sample S5 in Figure 4. Conversely, soils with lower metal concentrations (for example Fe, Ca, Zn in sample S2) is less influenced by moisture. Other factors such as organic matter (Ravansari and Lemke, 2018; Shand and Wendler, 2014; Weindorf et al., 2012), soil fertility (O'Rourke et al., 2016b; Sharma et al., 2015), texture, and density (Zhu et al., 2011) can also affect the XRF measurement.

Simple linear regression equations are adequate for fitting the data ($|r^2| > 0.8$) for certain elements (Fe, Zn, Zr, Rb, and Pb). However, these equations are not suitable for predicting concentrations in unknown soil samples because each chemical element in each soil exhibits a a unique evolution, with different equation, making it impossible to generalize the results.

To overcome this limitation, we calculated the relative decrease in concentrations (%) attributable to increasing soil moisture (Figure 5) and observed consistent decreases across five soil types. This consistency enables the modeling the entire data using a single exponential equation (Equation 1). The model accurately represents the trends for K, Fe, Zn, Rb, and Sr ($r^2 > 0.900$), and provided satisfactory results for the other elements (Figure 5). We categorized the elements into three groups based on their sensitivity to moisture: (i) low moisture-impacted concentrations (K, Ti, and Ca) - 70% of the concentration detected at 80% moisture, (ii) intermediate moisture-impacted concentrations (Fe, Pb, Zn, Zr, Rb, and Sr) - 50% of the concentration detected at 80% moisture, and (iii) high moisture-impacted concentrations (Mn) - only 25% of the concentration detected at 80% moisture. The results align with previous studies, albeit with minor variations (Padilla et al., 2019; Stockmann et al., 2016c). This effect of moisture on elementar concentration appears to be a reproducible and widely accepted phenomenon. For instance, Schneider et al. (2016) also employed exponential equations in their

241 modeling, and the coefficients of their equations were similar to those obtained in our study
242 (0.85 vs. 1.00, 0.90 vs. 0.87, and 0.93 vs. 0.95 for Fe, Pb, and Zn, respectively).

243 The measurement of XRF is influenced by the incoherent backscattering of the soil matrix
244 and composition, resulting in a Compton peak that affects XRF measurement accuracy (EPA
245 6200). Matrices containing lighter elements tend to produce higher Compton peaks. Instrument
246 calibration helps mitigate the effects of Compton scattering and minimize matrix effects, but
247 high soil moisture remains a challenge for accurate measurement. One of the primary effects of
248 mass in soils is the weight and dilution of the soil when water occupies the pore space (Mejía-
249 Piña et al., 2016). Hence, metal concentrations in moist soil should be expressed in mg kg_{moist}^{-1}
250 and the real concentration can be calculated using the following equation:

251 $$[M]_{dry\ soil} = [M]_{moist\ soil}.\ (1+U) \qquad \text{Equation 5}$$

252 Where

253 $[M]_{dry\ soil}$ is expressed in mg kg_{dry}^{-1}

254 $[M]_{dry\ soil}$ is expressed in mg kg_{moist}^{-1}

255 U is expressed in $kg_{water}\ kg_{dry\ soil}^{-1}$

256

257 This correction proves effective for certain elements. For Pb, Zn, Rb, and Sr (Supplementary
258 material, Figure S2), the concentrations only exhibit a slight decrease of 5.7% for Sr and 12.4%
259 for Zn at 80% soil moisture. However, for elements with lower atomic numbers like Fe, Mn, or
260 Cu, soil moisture continues to significantly impact the concentrations even after correction.
261 These elements have low electron binding energies, causing the emitted X-rays to be absorbed
262 and attenuated by water molecules. The mass attenuation coefficients for water and air are
263 higher for low-energy X-rays (Hubbell and Seltzer, 2009; Parsons et al., 2013).

264 Interestingly, K, Ca, and Ti, which are low atomic number elements belonging to period 4
265 and have lower energies of the characteristic Kα X-rays, showed an opposite trend (Figure S2).

Specifically, their corrected concentrations increased with higher moisture instead of decreasing. These elements are likely influenced by the intensity of the primary X-rays from the source enhanced by water (Ge et al., 2005). Padilla et al. (2019) found that the Compton Normalization method, suggested by some manufacturers to mitigate the adverse effect of moisture, was ineffective. Our findings underscore the necessity of a moisture correction independent of the instrument's internal correction and highlight the efficacy of the developed model (equation 4) over mass water corrections (equation 5).

Some authors in previous studies have suggested that soil moisture content should not exceed 20% when conducting soil parameters measurements (Kalnicky and Singhvi, 2001; Laiho and Perämäki, 2005; US Environmental Protection Agency, 2007). However, even at lower moisture levels, such as 10%, XRF concentration measurements are still significantly affected by moisture. Therefore, soil samples containing any moisture should be handled with caution. Some authors have noted that previous studies severely underestimated soil moisture (Mejía-Piña et al., 2016; Parsons et al., 2013; Stockmann et al., 2016b) and recommended minimal moisture when conducting soil investigation. Soil moisture has such a severe effect on analysis that Mejia-Pia et al. (2016) mentioned a maximum threshold of 5% and even advised measuring moisture in dry soil after a long storage period (Mejía-Piña et al., 2016). With the model developed in this study, the systematic moisture correction from XRF measurement errors eliminates this limitation and provides much more precise results in any **circumstance**.

3.3. *Correction of geochemical field maps using the model*

Geochemical field mapping was carried out over several days in varying weather conditions in Portugal and France. As the mapping during the missions had to continue even after rain events or during light rain, the soil was sometimes drier and sometimes wetter during the pXRF measurements. Therefore, soil moisture was estimated using the general final model (Equation 4), and the geochemical soil maps were generated with and without moisture correction (Figure

6, S3 and S7). As expected, a disparity between the two maps emerged in Estarreja (Portugal), particularly in the lowlands southwestern region near the coast where the soils were more humid (Figure 6C). Despite the sunny conditions, with soil moisture generally below 30%, the geochemical investigation by pXRF measurements underestimated the concentrations of Fe, Zn, and Pb by 32.1%, 29.5%, and 21.4%, respectively (Table 2).

During field mapping in the Pyrenean OHM (Vicdessos), the conditions were more humid, with the average soil moisture at 53%, twice the mean value observed in the Portuguese soils (Supplementary material, Figures S6 and S7). This results in greater differences between corrected and uncorrected geochemical maps. In such humid mountainous conditions, the moisture effect considerably biased the XRF measurements, leading to an error of more than 50% fro Fe and Zn (Table 2).

Stockmann et al. (2016) also produced maps of Fe before and after correction for soil moisture, using a linear equation between Fe (air-dried) and Fe (field-wet) to create a model for estimating soil content, assuming homogeneous soil moisture. However, this assumption is not applicable in some situations, particularly in scenarios where XRF data are collected at different sampling dates, over several days, under different moisture conditions, or across different landscape units such as well-drained plateaus, hill slopes, flood plains, etc.

Soil moisture poses a primary challenge for accurate geochemical field mapping. Its influence is significant enough that certain researchers have explored the possibility of integrating a soil moisture sensor into the pXRF analyzer (Potts and West, 2008; Ravansari and Lemke, 2018). The method proposed in our study represents a novel approach capable of effectively eliminating the moisture effect in geochemical field mapping without incurring additional costs.

4. Conclusion

The limitations imposed by soil moisture on *in situ* XRF analysis can be overcome through the utilization of a predictive model constructed in two steps, enabling the estimation of of soil moisture directly from XRF measurements with a high accuracy of 98%. This innovative method offers a reliable solution for successful *in situ* XRF analysis and represents a significant advancement in environmental research. The two-step process involves first estimating soil moisture from *in situ* XRF measurement errors, followed by the correction of XRF measurements for moisture. Through this post-processing method, the accuracy of geochemical field maps is considerably enhanced, with differences in metal concentration before and after correction exceeding 50%. It facilitates the extensive utilization of portable XRF instruments in various environments, delivering precise and comparable results across different ecosystems, climatic conditions and collection times. In summary, our approach offers a cost-effective and efficient solution to mitigate the impact of soil moisture on *in situ* XRF analysis, thereby holding consirable potential for advancing environmental soil research.

Acknowledgments

The project has been funded by the CNRS TRAM Project (ANR-15-CE01-0008) and Observatoire Homme-Milieu Pyrénées Haut Vicdessos - LABEX DRIIHM ANR-11-LABX0010. The research was also funded by FCT (Fundação para a Ciência e a Tecnologia, Portugal) through projects UIDB/04683/2020, UIDP/04683/2020 (Institute of Earth Sciences, pole of University of Minho). We extend our sincere gratitude to the scientific teams at the Laboratoire Ecologie Fonctionnelle et Environnement (ECOLAB - UMR 5245 CNRS-UT3-INPT) and of the Laboratoire Geographie de l´Environnement (GEODE - UMR 5602 CNRS-UT2J) in Toulouse, France, for their invaluable assistance, both analytically and financially.

We are also acknowledge the Universidade Federal do Recôncavo da Bahia, Brazil, for providing salary support to the first author during one year for research.

References

Akopyan, K., Petrosyan, V., Grigoryan, R., Melkomian, D.M., 2018. Assessment of residential soil contamination with arsenic and lead in mining and smelting towns of northern Armenia. J. Geochemical Explor. 184, 97–109. https://doi.org/10.1016/j.gexplo.2017.10.010

Argyraki, A., Ramsey, M.H., Potts, P.J., 1997. Evaluation of Portable X-ray Fluorescence Instrumentation for in situ Measurements of Lead on Contaminated Land. Analyst 122, 743–749. https://doi.org/10.1039/A700746I

Barradas, J.M., Cardoso Fonseca, E., Ferreira da Silva, E., Garcia Pereira, H., 1992. Identification and mapping of pollution indices using a multivariate statistical methodology, Estarreja, central Portugal. Appl. Geochemistry 7, 563–572. https://doi.org/10.1016/0883-2927(92)90071-A

Bastos, R.O., Melquiades, F.L., Biasi, G.E. V, 2012. Correction for the effect of soil moisture on in situ XRF analysis using low-energy background. X-Ray Spectrom. 41, 304–307. https://doi.org/10.1002/xrs.2397

Benedet, L., Faria, W.M., Silva, S.H.G., Mancini, M., Demattê, J.A.M., Guilherme, L.R.G., Curi, N., 2020. Soil texture prediction using portable X-ray fluorescence spectrometry and visible near-infrared diffuse reflectance spectroscopy. Geoderma 376. https://doi.org/10.1016/j.geoderma.2020.114553

Borges, C.S., Weindorf, D.C., Nascimento, D.C., Curi, N., Guilherme, L.R.G., Carvalho, G.S., Ribeiro, B.T., 2020. Comparison of portable X-ray fluorescence spectrometry and laboratory-based methods to assess the soil elemental composition: Applications for wetland soils. Environ. Technol. Innov. 19, 100826. https://doi.org/10.1016/j.eti.2020.100826

Caporale, A.G., Adamo, P., Capozzi, F., Langella, G., Terribile, F., Vingiani, S., 2018. Monitoring metal pollution in soils using portable-XRF and conventional laboratory-based techniques: Evaluation of the performance and limitations according to metal properties and sources. Sci. Total Environ. 643, 516–526. https://doi.org/10.1016/j.scitotenv.2018.06.178

Costa, C., Jesus-Rydin, C., 2001. Site investigation on heavy metals contaminated ground in Estarreja - Portugal. Eng. Geol. 60, 39–47. https://doi.org/10.1016/S0013-7952(00)00087-9

De La Calle, I., Cabaleiro, N., Romero, V., Lavilla, I., Bendicho, C., 2013. Sample pretreatment strategies for total reflection X-ray fluorescence analysis: A tutorial review. Spectrochim. Acta Part B At. Spectrosc. 90, 23–54. https://doi.org/10.1016/J.SAB.2013.10.001

Ge, L., Lai, W., Lin, Y., 2005. Influence of and correction for moisture in rocks, soils and sediments on in situ XRF analysis. X-Ray Spectrom. 34, 28–34.

https://doi.org/10.1002/xrs.782

Goovaerts, P., 1999. Geostatistics in soil science: State-of-the-art and perspectives. Geoderma 89, 1–45. https://doi.org/10.1016/S0016-7061(98)00078-0

Hansson, S. V, Claustres, A., Probst, A., De Vleeschouwer, F., Baron, S., Galop, D., Mazier, F., Le Roux, G., 2017. Atmospheric and terrigenous metal accumulation over 3000 years in a French mountain catchment: Local vs distal influences. Anthropocene 19, 45–54. https://doi.org/10.1016/j.ancene.2017.09.002

Hansson, S. V, Grusson, Y., Chimienti, M., Claustres, A., Jean, S., Le Roux, G., 2019. Legacy Pb pollution in the contemporary environment and its potential bioavailability in three mountain catchments. Sci. Total Environ. 671, 1227–1236. https://doi.org/https://doi.org/10.1016/j.scitotenv.2019.03.403

Horta, A., Azevedo, L., Neves, J., Soares, A., Pozza, L., 2021. Integrating portable X-ray fluorescence (pXRF) measurement uncertainty for accurate soil contamination mapping. Geoderma 382, 114712. https://doi.org/10.1016/j.geoderma.2020.114712

Hubbell, J.H., Seltzer, S.M., 2009. X-Ray Mass Attenuation Coefficients | NIST [WWW Document]. URL https://www.nist.gov/pml/x-ray-mass-attenuation-coefficients (accessed 9.22.18).

Inácio, M., Neves, O., Pereira, V., Ferreira da Silva, E., 2014. Levels of selected potential harmful elements (PHEs) in soils and vegetables used in diet of the population living in the surroundings of the Estarreja Chemical Complex (Portugal). Appl. Geochemistry 44, 38–44. https://doi.org/10.1016/j.apgeochem.2013.07.017

Inácio, M.M., Pereira, V., Pinto, M.S., 1998. Mercury contamination in sandy soils surrounding an industrial emission source (Estarreja, Portugal). Geoderma 85, 325–339. https://doi.org/10.1016/S0016-7061(98)00027-5

Kallithrakas-Kontos, N., Foteinis, S., Paigniotaki, K., Papadogiannakis, M., 2016. A robust X-ray fluorescence technique for multielemental analysis of solid samples. Environ. Monit. Assess. 188, 1–10. https://doi.org/10.1007/s10661-016-5127-4

Kalnicky, D.J., Singhvi, R., 2001. Field portable XRF analysis of environmental samples. J. Hazard. Mater. 83, 93–122. https://doi.org/10.1016/S0304-3894(00)00330-7

Laiho, J.V.-P., Perämäki, P., 2005. Evaluation of portable X-ray fluorescence (PXRF) - Sample preparation methods. Geol. Surv. Finl. 38, 73–82.

Lemière, B., 2018. A review of pXRF (fi eld portable X-ray fl uorescence) applications for applied geochemistry. J. Geochemical Explor. 188, 350–363. https://doi.org/10.1016/j.gexplo.2018.02.006

Li, F., Xu, L., You, T., Lu, A., 2021. Measurement of potentially toxic elements in the soil through NIR, MIR, and XRF spectral data fusion. Comput. Electron. Agric. 187, 106257. https://doi.org/https://doi.org/10.1016/j.compag.2021.106257

Marinho-reis, A.P., Costa, C., Rocha, F., Cave, M., Wragg, J., Valente, T., Sequeira-braga, A., Noack, Y., 2020. Biogeochemistry of household dust samples collected from private homes of a portuguese industrial city. Geosci. 10, 1–20. https://doi.org/10.3390/geosciences10100392

Mejía-Piña, K.G., Huerta-Diaz, M.A., González-Yajimovich, O., 2016. Calibration of handheld

X-ray fluorescence (XRF) equipment for optimum determination of elemental concentrations in sediment samples. Talanta 161, 359–367. https://doi.org/10.1016/j.talanta.2016.08.066

Nawar, S., Richard, F., Kassim, A.M., Tekin, Y., Mouazen, A.M., 2022. Fusion of Gamma-rays and portable X-ray fluorescence spectral data to measure extractable potassium in soils. Soil Tillage Res. 223, 105472. https://doi.org/https://doi.org/10.1016/j.still.2022.105472

O'Rourke, S.M., Stockmann, U., Holden, N.M., McBratney, A.B., Minasny, B., 2016a. An assessment of model averaging to improve predictive power of portable vis-NIR and XRF for the determination of agronomic soil properties. Geoderma 279, 31–44. https://doi.org/10.1016/J.GEODERMA.2016.05.005

O'Rourke, S.M., Stockmann, U., Holden, N.M., McBratney, A.B., Minasny, B., 2016b. An assessment of model averaging to improve predictive power of portable vis-NIR and XRF for the determination of agronomic soil properties. Geoderma 279, 31–44. https://doi.org/10.1016/j.geoderma.2016.05.005

Padilla, J.T., Hormes, J., Magdi Selim, H., 2019. Use of portable XRF: Effect of thickness and antecedent moisture of soils on measured concentration of trace elements. Geoderma 337, 143–149. https://doi.org/10.1016/j.geoderma.2018.09.022

Parsons, C., Grabulosa, E.M., Pili, E., Floor, G.H., Roman-Ross, G., Charlet, L., 2013. Quantification of trace arsenic in soils by field-portable X-ray fluorescence spectrometry: Considerations for sample preparation and measurement conditions. J. Hazard. Mater. 262, 1213–1222. https://doi.org/10.1016/j.jhazmat.2012.07.001

Plumejeaud, S., Reis, A.P., Tassistro, V., Patinha, C., Noack, Y., Orsière, T., 2018. Potentially harmful elements in house dust from Estarreja, Portugal: characterization and genotoxicity of the bioaccessible fraction. Environ. Geochem. Health 40, 127–144. https://doi.org/10.1007/s10653-016-9888-z

Potts, P.J., West, M., 2008. Portable x-ray fluorescence spectrometry : capabilities for in situ analysis, Royal Soci. ed. Cambridge.

Qingya, W., Li, F., Jiang, X., Hao, J., Zhao, Y., Wu, S., Cai, Y., Huang, W., 2022. Quantitative analysis of soil cadmium content based on the fusion of XRF and Vis-NIR data. Chemom. Intell. Lab. Syst. 226, 104578. https://doi.org/https://doi.org/10.1016/j.chemolab.2022.104578

Qu, M., Guang, X., Liu, H., Zhao, Y., Huang, B., 2022. Additional sampling using in-situ portable X-ray fluorescence (PXRF) for rapid and high-precision investigation of soil heavy metals at a regional scale. Environ. Pollut. 292, 118324. https://doi.org/https://doi.org/10.1016/j.envpol.2021.118324

Ravansari, R., Lemke, L.D., 2018. Portable X-ray fluorescence trace metal measurement in organic rich soils: pXRF response as a function of organic matter fraction. Geoderma 319, 175–184. https://doi.org/10.1016/j.geoderma.2018.01.011

Ravansari, R., Wilson, S.C., Tighe, M., 2020. Portable X-ray fluorescence for environmental assessment of soils: Not just a point and shoot method. Environ. Int. 134, 105250. https://doi.org/10.1016/j.envint.2019.105250

Rouillon, M., Taylor, M.P., 2016. Can field portable X-ray fluorescence (pXRF) produce high

quality data for application in environmental contamination research? Environ. Pollut. 214, 255–264. https://doi.org/10.1016/J.ENVPOL.2016.03.055

Schneider, A.R., Cancès, B., Breton, C., Ponthieu, M., Morvan, X., Conreux, A., Marin, B., 2016. Comparison of field portable XRF and aqua regia/ICPAES soil analysis and evaluation of soil moisture influence on FPXRF results. J. Soils Sediments. https://doi.org/10.1007/s11368-015-1252-x

Shand, C.A., Wendler, R., 2014. Portable X-ray fluorescence analysis of mineral and organic soils and the influence of organic matter. J. Geochemical Explor. 143, 31–42. https://doi.org/10.1016/j.gexplo.2014.03.005

Sharma, A., Weindorf, D.C., Man, T., Abdalsatar, A., Aldabaa, A., Chakraborty, S., 2014. Characterizing soils via portable X-ray fluorescence spectrometer: 3. Soil reaction (pH). Geoderma 232–234, 141–147. https://doi.org/10.1016/j.geoderma.2014.05.005

Sharma, A., Weindorf, D.C., Wang, D., Chakraborty, S., 2015. Characterizing soils via portable X-ray fluorescence spectrometer: 4. Cation exchange capacity (CEC). Geoderma 239–240, 130–134. https://doi.org/10.1016/j.geoderma.2014.10.001

Shrestha, G., Calvelo-Pereira, R., Roudier, P., Martin, A.P., Turnbull, R.E., Kereszturi, G., Jeyakumar, P., Anderson, C.W.N., 2022. Quantification of multiple soil trace elements by combining portable X-ray fluorescence and reflectance spectroscopy. Geoderma 409, 115649. https://doi.org/https://doi.org/10.1016/j.geoderma.2021.115649

Simonneau, A., Chapron, E., Courp, T., Tachikawa, K., Le Roux, G., Baron, S., Galop, D., Garcia, M., Di Giovanni, C., Motellica-Heino, M., Mazier, F., Foucher, A., Houet, T., Desmet, M., Bard, E., 2013. Recent climatic and anthropogenic imprints on lacustrine systems in the Pyrenean Mountains inferred from minerogenic and organic clastic supply (Vicdessos valley, Pyrenees, France). Holocene 23, 1764–1777. https://doi.org/10.1177/0959683613505340

Stockmann, U., Cattle, S.R., Minasny, B., McBratney, A.B., 2016a. Utilizing portable X-ray fluorescence spectrometry for in-field investigation of pedogenesis. Catena 139, 220–231. https://doi.org/10.1016/j.catena.2016.01.007

Stockmann, U., Jang, H.H., Minasny, B., McBratney, A.B., 2016b. The Effect of Soil Moisture and Texture on Fe Concentration Using Portable X-Ray Fluorescence Spectrometers, in: Digital Soil Morphometrics. pp. 63–71. https://doi.org/10.1007/978-3-319-28295-4

Stockmann, U., Jang, H.J., Minasny, B., McBratney, A.B., 2016c. The effect of soil moisture and texture on Fe concentration using portable X-Ray fluorescence spectrometers, in: Digital Soil Morphometrics. pp. 63–71.

US Environmental Protection Agency, 2007. Method 6200 : Field portable X-ray fluorescence spectrometryfor the determination of elemental concentrations in soil and sediment, Test Methods For Evaluating Solid Waste, US Environmental Protection Agency. https://doi.org/10.1017/CBO9781107415324.004

Weindorf, D.C., Bakr, N., Zhu, Y., 2014. Advances in portable X-ray fluorescence (PXRF) for environmental, pedological, and agronomic applications. Adv. Agron. 128. https://doi.org/10.1016/B978-0-12-802139-2.00001-9

Weindorf, D.C., Zhu, Y., Mcdaniel, P., Valerio, M., Lynn, L., Michaelson, G., Clark, M., Ping, C.L., 2012. Characterizing soils via portable x-ray fluorescence spectrometer: 2. Spodic

508 and Albic horizons. Geoderma 189–190, 268–277.
509 https://doi.org/10.1016/j.geoderma.2012.06.034

510 Young, K.E., Evans, C.A., Hodges, K. V., Bleacher, J.E., Graff, T.G., 2016. A review of the
511 handheld X-ray fluorescence spectrometer as a tool for field geologic investigations on
512 Earth and in planetary surface exploration. Appl. Geochemistry 72, 77–87.
513 https://doi.org/10.1016/j.apgeochem.2016.07.003

514 Zhu, Y., Weindorf, D.C., Zhang, W., 2011. Characterizing soils using a portable X-ray
515 fluorescence spectrometer: 1. Soil texture. Geoderma 167–177.
516 https://doi.org/10.1016/j.geoderma.2011.08.010

Table 1
Statistical summary of the multiple regression model for estimating soil moisture from measurement errors obtained during X-ray fluorescence (XRF) spectrometry analysis.

Analysis of variance	*Degree of freedom*	*Sum Squares*	*Mean Squares*	*F*	*Critical value F*
Regression	15	3.3317	0.2220	159.37	5.94E-50
Residus	74	0.1034	0.0013		
Total	89	3.4342			

Regression statistics	
Multiple coefficient of determination	0.9848
Coefficient of determination	0.9699
Error	0.0373
Observations	75

Coefficient of the regression	
Constant	0.0939
Cr Error	0.0935
As Error	0.1291
Zn Error	0.0392
V Error	0.0439
S Error	0.0005
Ti Error	-0.0002
K Error	-0.0055
Co Error	-0.0294
Fe Error	0.0099
Sc Error	0.0084
Ca Error	-0.0053
Pb Error	-0.1392
Rb Error	0.1435
Zr Error	0.0780
Sr Error	-0.3694

Table 2
Mean concentrations of Fe, Zn and Pb in soil samples before and after soil moisture correction, in the in situ entire XRF datasets at the OHM in Estarreja (Portugal) and the OHM in Vicdessos (France).

	OHM Estarreja	*OHM Vicdessos*
Number of samples	140	95
Mean moisture (± SD)	27 % (± 20%)	53 % (± 18%)
Mean [Fe] before correction (mg kg^{-1})	11,200	20,600
Mean [Fe] after correction (mg kg^{-1})	14,800	32,100
Difference due to moisture effect (%)	***32.1***	***55.8***
Mean [Zn] before correction (mg kg^{-1})	61	92
Mean [Zn] after correction (mg kg^{-1})	79	142
Difference due to moisture effect (%)	***29.5***	***54.3***
Mean [Pb] before correction (mg kg^{-1})	28	18
Mean [Pb] after correction (mg kg^{-1})	34	26
Difference due to moisture effect (%)	***21.4***	***44.4***

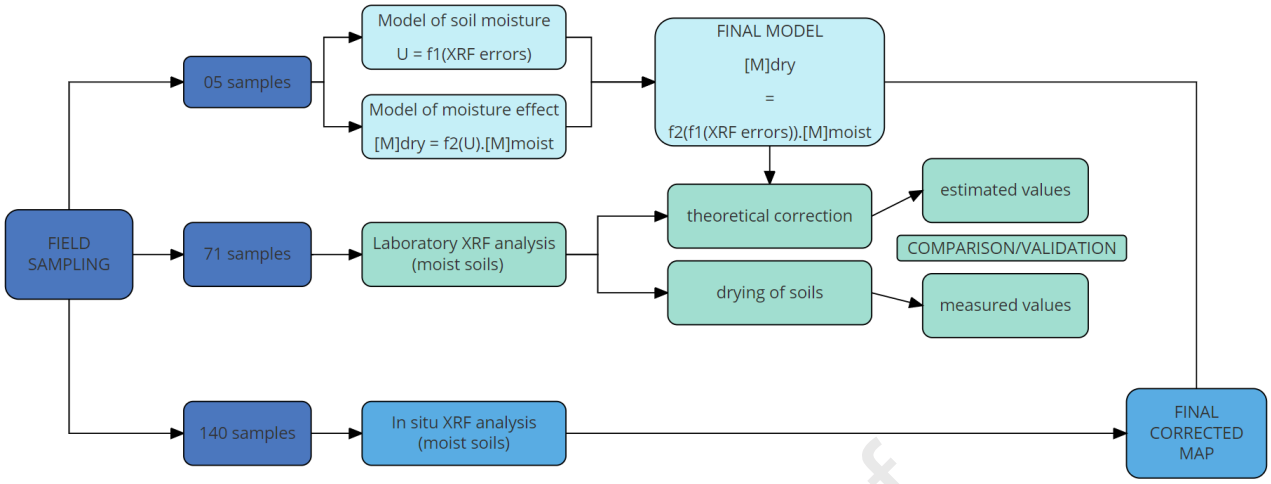

Fig. 1. Methodology flow chart for correcting geochemical XRF field data using soil moisture modeling.

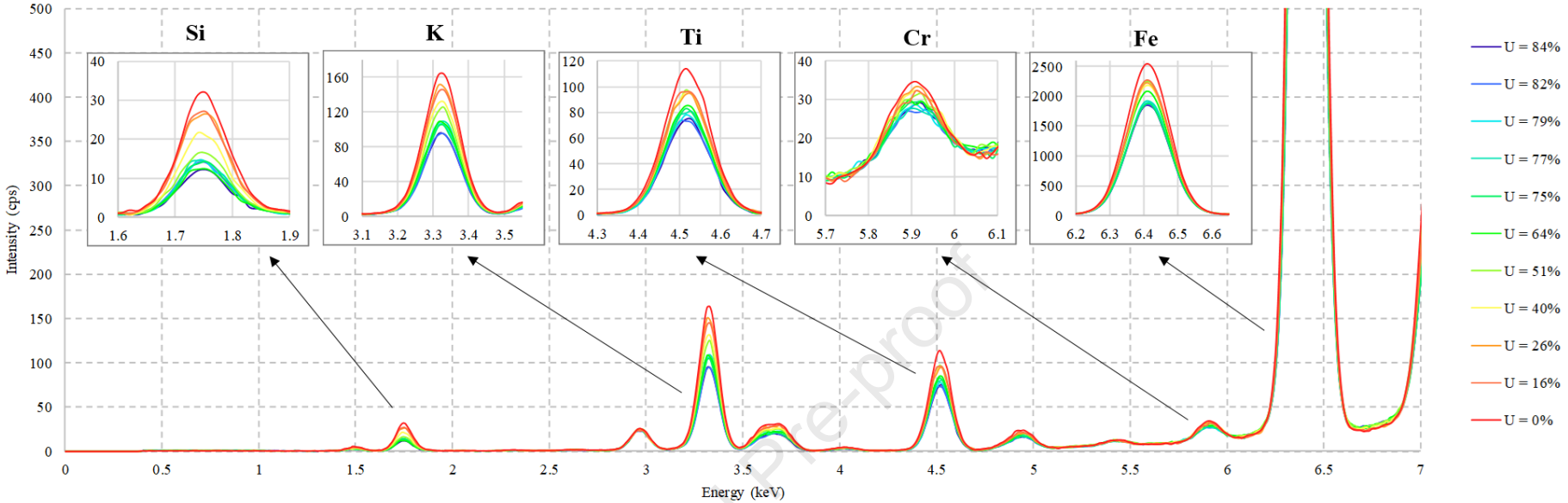

Fig. 2. Evolution of XRF spectra during the drying of soil sample S2 from 84% to 0% gravimetric moisture in Experiment 1.

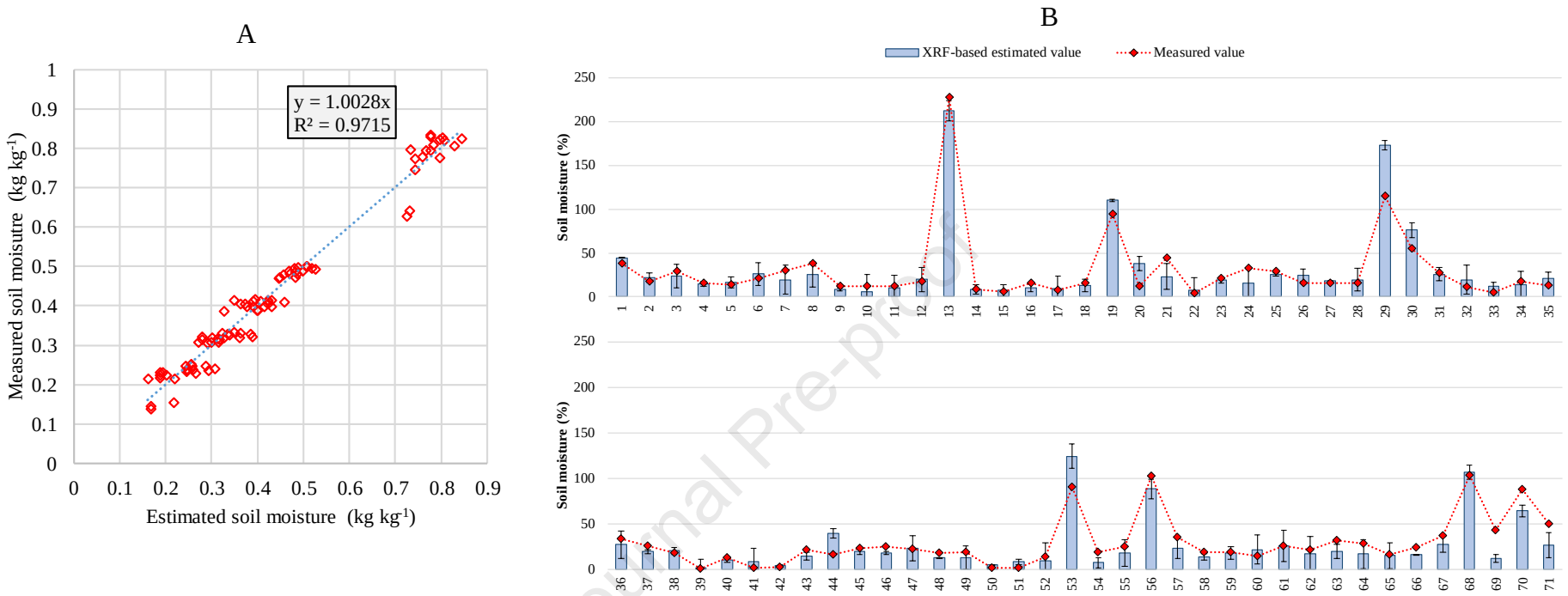

Fig. 3. Comparison of measured moisture values with moisture values estimated from modeling based on XRF errors (A) in laboratory conditions and (B) in 71 different soil samples from Portugal.

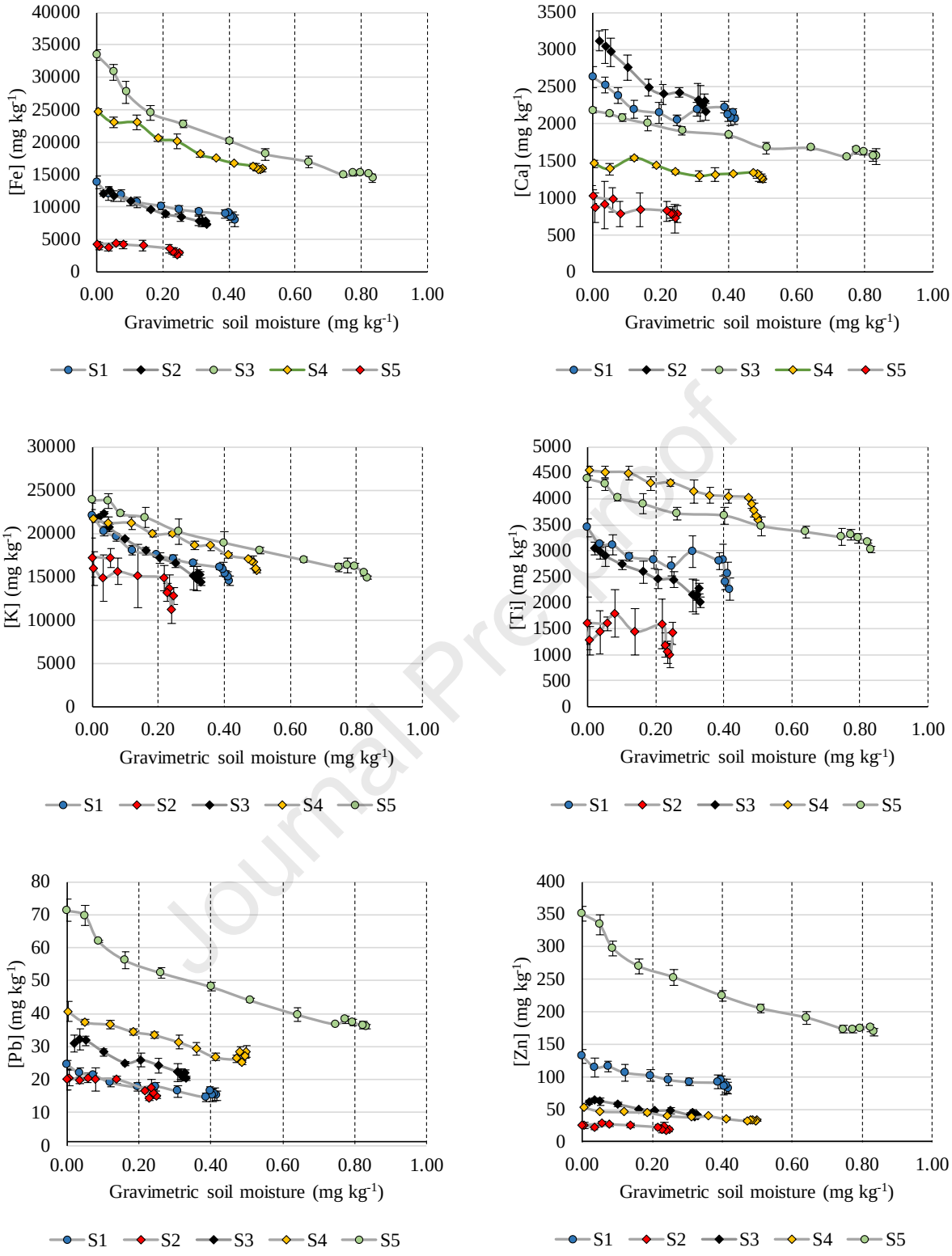

Fig. 4. Mean total concentrations of Fe, Ca, K, Ti, Pb and Zn in five soils with different moisture conditions during the Experiment 1.

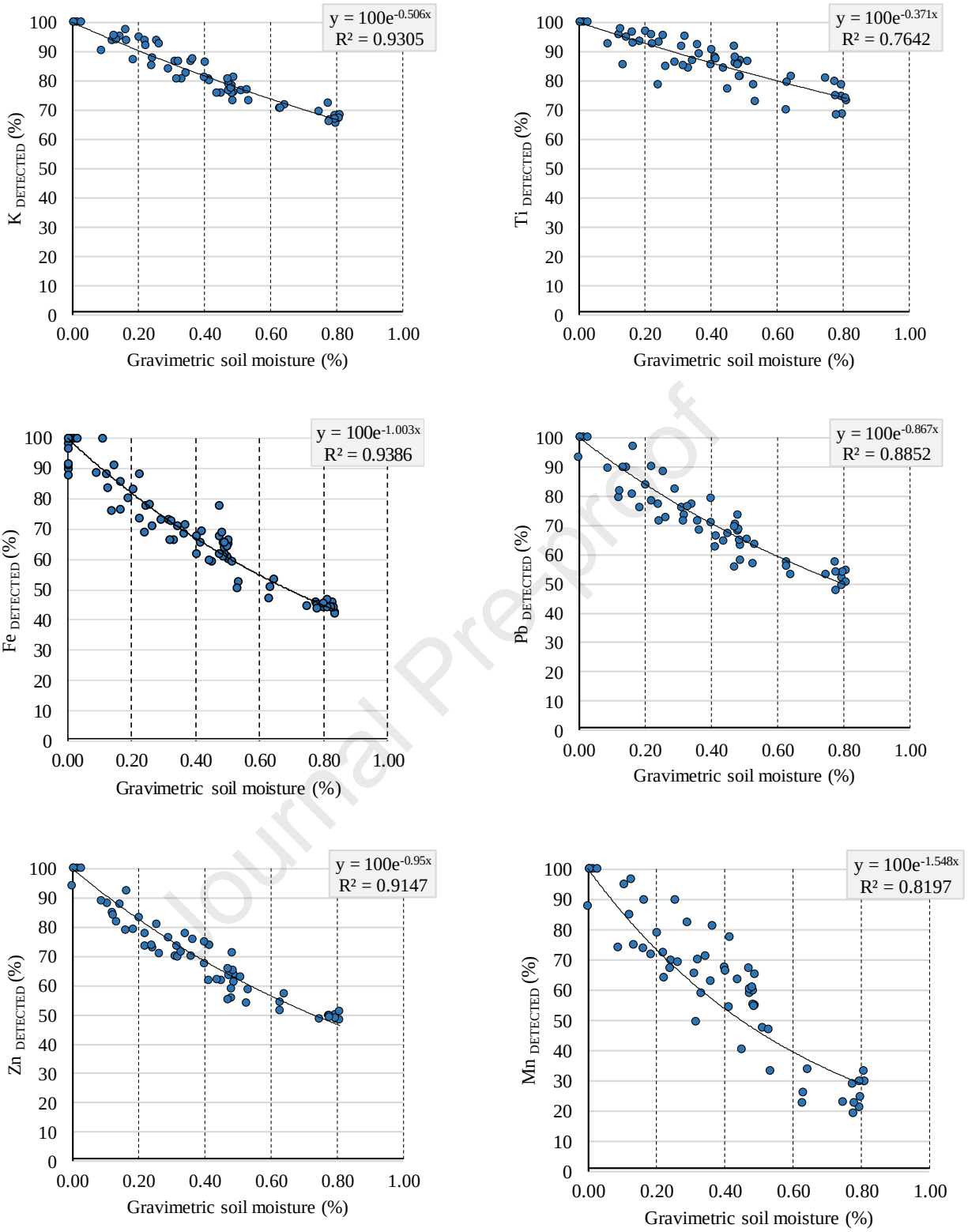

Fig. 5. Proportion of detection of K, Ti, Fe, Pb, Zn and Mn (%) in the five soil samples according to soil moisture, using X-ray fluorescence spectrometry.

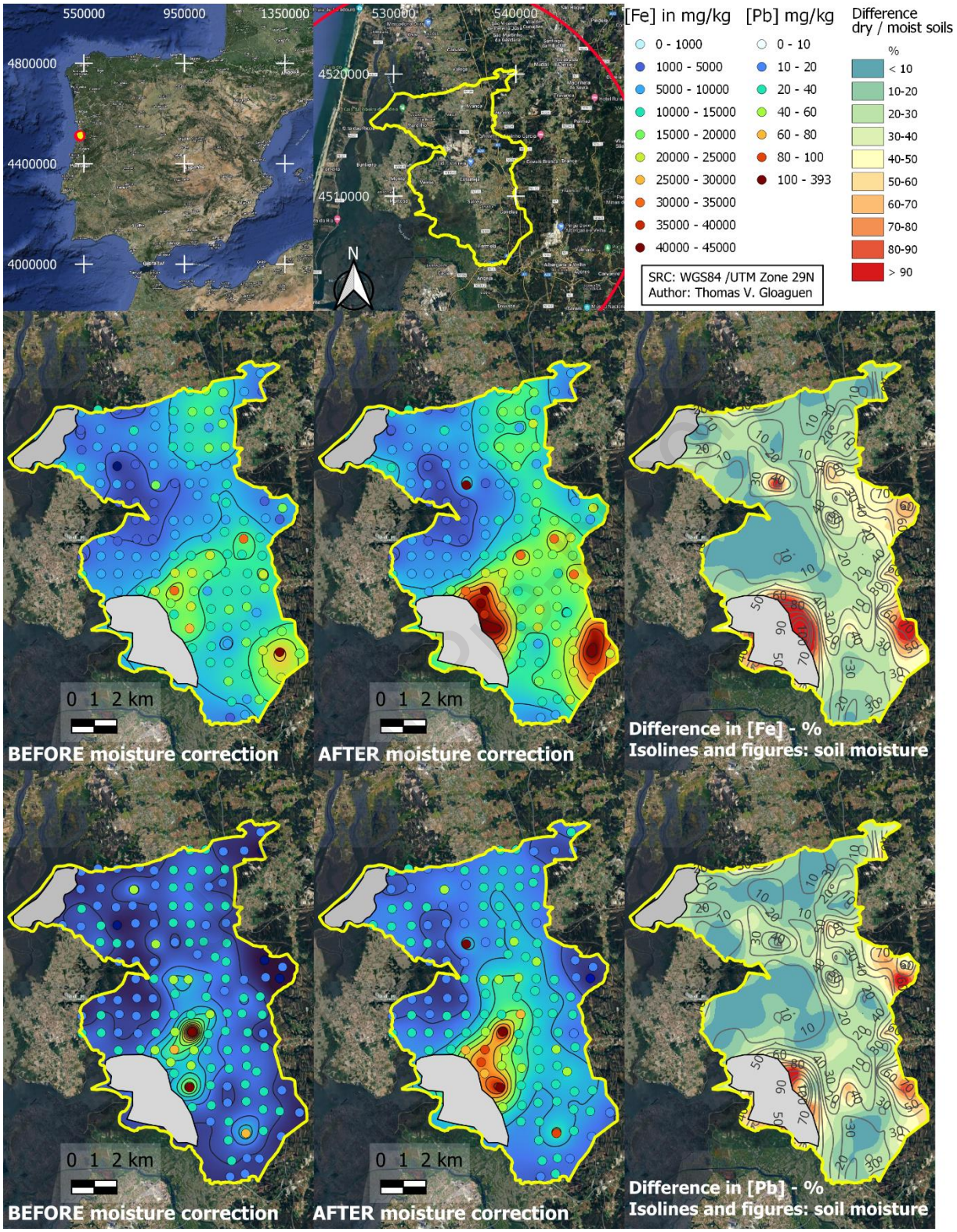

Fig. 6. Maps of concentration of Fe and Pb before moisture correction (first map), after moisture correction (second map) and difference (%) between concentrations according to soil moisture (third map) in superficial soils obtained from in situ XRF data, at OHM Estarreja, Portugal.

Highlights

- The soil moisture was modeled directly from field pXRF data.
- The accuracy of the predictive model exceeded 98%.
- Correction of Fe, Pb or Zn maps prevented mean errors of up to 50%.
- The estimation of moisture requires no additional data acquisition.
- The method allows geochemical mapping under variable climatic conditions.

Declaration of interests

☒ The authors declare that they have no known competing financial interests or personal relationships that could have appeared to influence the work reported in this paper.

☐The authors declare the following financial interests/personal relationships which may be considered as potential competing interests: